Breast Cancer Research

RESEARCH

Open Access

Neutrophil extracellular traps induced by neoadjuvant chemotherapy of breast cancer promotes vascular endothelial damage

Linghui Kong[1†], Song Hu[1†], Ying Zhao[1†], Yan Huang[1], Xiaobing Xiang[1], Yang Yu[2], Xiaochun Mao[3], Kangjie Xie[1], Xiaoyan Zhu[4] and Pingbo Xu[1*]

Abstract

Background The mechanisms underpinning neoadjuvant chemotherapy-induced vascular endothelial injury in breast cancer remain elusive. Our study aims to demonstrate that Neutrophil Extracellular Traps (NETs) play a pivotal role in neoadjuvant chemotherapy-induced vascular endothelial injury in breast cancer, elucidating that chemotherapy-induced upregulation of *Solute Carrier 11a1* (*Slc11a1*) modulates Reactive Oxygen Species (ROS) generation, which may be critical for NETs formation.

Methods We investigated the impact of neoadjuvant chemotherapy for breast cancer on NETs formation and vascular endothelial injury by analyzing NETs dsDNA and serum markers in patients, cells, and chemotherapy mouse models. RNA sequencing of neutrophils from chemotherapy mouse models was performed to identify the potential NETs formation-associated gene *Slc11a1*, which was further validated through cellular and animal experiments by assessing *Slc11a1* expression, intracellular ferrous ion content, and ROS levels. Knockdown of *Slc11a1* in human neutrophils and mouse models were also performed to further confirm the phenotypic results.

Results Our study revealed that plasma NETs formation and endothelial injury markers were significantly elevated in breast cancer patients undergoing docetaxel & carboplatin (TCb) neoadjuvant chemotherapy, compared to controls. In these patients, NETs formation was associated with the augmentation of endothelial injury markers. Chemotherapy mouse models demonstrated that TCb treatment markedly elevated NETs formation and endothelial injury, which can be mitigated by Cl-amidine, a protein-arginine deiminase inhibitor. In human neutrophils, we demonstrated that the TCb chemotherapeutic agents (combination of docetaxel and carboplatin) induced the formation of NETs, which subsequently facilitated damage to human umbilical vein endothelial cells in vitro. RNA sequencing of mouse neutrophils identified *Slc11a1* as a key NETs formation-related gene, which was upregulated by TCb chemotherapy in neutrophils, leading to increased intracellular ferrous ion content and ROS generation. Knockdown of *Slc11a1* in human neutrophils and mouse models demonstrated its reversal effect on TCb-induced ferrous ion upregulation, ROS generation, and NETs formation.

Conclusions Our research underscores the capacity of TCb neoadjuvant chemotherapy in breast cancer to augment NETs formation in neutrophils through *Slc11a1*-mediated ROS generation, which is linked to vascular endothelial injury. Our study elucidates the potential mechanisms underlying perioperative vascular endothelial injury in breast

[†]Linghui Kong, Song Hu and Ying Zhao have contributed equally to this work.

*Correspondence:
Pingbo Xu
zzmzkxpb@163.com
Full list of author information is available at the end of the article

cancer patients undergoing neoadjuvant chemotherapy, offering novel insights into perioperative therapeutic management strategies for these patients.

Keywords Neoadjuvant chemotherapy, Neutrophil extracellular traps, Vascular endothelial cells, Reactive oxygen species, Solute carrier 11a1

Background

Neoadjuvant chemotherapy occupies a pivotal position in preoperative breast cancer management, particularly for HER2-positive and triple-negative subtypes [1]. However, chemotherapy is recognized as a significant risk factor for vascular injury and thrombosis, increasing the risk by up to 6.5-fold beyond tumor-intrinsic factors [2]. Neoadjuvant chemotherapy prior to surgery significantly elevates the risk of perioperative vascular injury in breast cancer patients, with the baseline risk of thrombosis due to vascular injury being < 1% but escalating to 5–17% post-chemotherapy [3]. Vascular endothelial injury-induced coagulation disorders constitute a significant perioperative safety threat, leading to hypercoagulability, thrombosis, and subsequent adverse events such as pulmonary embolism, cerebral infarction, and myocardial infarction [4]. Yet, the mechanisms underlying neoadjuvant chemotherapy-induced vascular endothelial injury in breast cancer remain elusive, representing a tangible obstacle to meticulous perioperative management. Thus, a profound understanding of these mechanisms is essential for preventing perioperative coagulation disorders and enhancing the quality of life during the perioperative period for breast cancer patients.

Vascular endothelial cells engage directly with various immune cells circulating in the bloodstream. Studies have emphasized the close relationship between the hyperactivation of immune cells, particularly neutrophils, and the occurrence of vascular endothelial injury [5]. Neutrophils mediate tissue damage and inflammation, with activated subsets releasing their nuclear contents through Neutrophil Extracellular Traps (NETs) — DNA structures adorned with cytoplasmic and granular proteins [6]. The release of NETs elicits endothelial injury and activation, provoking inflammation [7]. NETs formation is influenced by diverse stimuli, including activation by inflammatory cytokines such as IL-8 and TNF-α, which leads neutrophils to generate reactive oxygen species (ROS) that trigger downstream events like histone modifications and chromatin decondensation [8]. ROS activate peptidylarginine deiminase (PAD) 4, which inverts arginine residues on histones to citrulline and loosens chromatin structure [9]. This decondensed chromatin combines with cytoplasmic proteins such as Myeloperoxidase (MPO) and is expelled through ruptured membranes, and forming NETs [10]. Notably, breast cancer neoadjuvant chemotherapy impairs the immune system, including neutrophils, as evidenced by a 2023 study by Mousset et al. that revealed NETs formation and accumulation post-chemotherapy, strongly associated with poor prognosis [11]. A study suggests that breast cancer chemotherapy generates toxic ROS to induce tumor cell apoptosis [12], potentially prompting neutrophils to release NETs. However, whether and how breast cancer neoadjuvant chemotherapy triggers NETs activation and the subsequent NETs-mediated endothelial injury remains underexplored and necessitates further evidence.

In this study, we will demonstrate that NETs play a pivotal role in neoadjuvant chemotherapy-induced vascular endothelial injury in breast cancer through an integrated approach that encompasses investigations involving breast cancer neoadjuvant chemotherapy patients, neoadjuvant chemotherapy mouse models, and in vitro cultures of neutrophils. Through these approaches, we will elucidate the chemotherapy's promotion of NETs formation and subsequent endothelial damage. Furthermore, by leveraging RNA sequencing, we will identify the Solute Carrier 11a1 (*Slc11a1*) gene as being linked to chemotherapy-mediated NETs formation. We will employ *Slc11a1* knockdown approaches in both human neutrophils and neoadjuvant chemotherapy mouse models, thereby confirming that chemotherapy-induced upregulation of *Slc11a1* facilitates NETs generation through augmented ROS production in neutrophils.

Methods

Patients and blood sample assessment

This study included patients undergoing breast surgery at Zhejiang Cancer Hospital between September 2023 and June 2024. Eligibility criteria included individuals aged between 18 and 80 years, who had undergone either neoadjuvant chemotherapy prior to surgery or none, and were scheduled for either a mastectomy or breast-conserving surgery. Patients were excluded based on the following criteria: a history of any other malignancy, documented coagulation disorders or anticoagulant use, long-term oral contraceptive use, and male breast cancer. Upon enrollment, patients were categorized into four distinct groups based on the neoadjuvant chemotherapy

regimen they had received prior to surgery. The normal control group (NC), where patients did not receive standard neoadjuvant chemotherapy regimens prior to surgery; the epirubicin & cyclophosphamide—taxol (EC-T) group, where patients received epirubicin and cyclophosphamide for four cycles, followed by docetaxel for four cycles prior to surgery; the epirubicin & cyclophosphamide—taxol with Herceptin & Perjeta (EC-T-HP) group, where patients received chemotherapy regimens incorporating Herceptin and Perjeta into each cycle based on EC-T; the docetaxel & carboplatin (TCb) group, where patients received docetaxel and carboplatin for eight cycles prior to surgery. On the day of surgery, prior to anesthesia induction, 10 mL of peripheral venous blood was collected from each patient and subjected to centrifugation. The plasma was then analyzed for the quantification of free double-stranded DNA (dsDNA) using the Quant-It PicoGreen® dsDNA Assay Kit (Thermo Fisher Scientific, USA; Catalog No. P11495) [13, 14]. Additionally, the concentrations of MPO, histone H3, von Willebrand Factor (vWF), and Syndecan-4 in the plasma were measured using enzyme-linked immunosorbent assay (ELISA) kits (Kepeirui, China; Catalog Nos. H10141, H13742, H10950, and H18626, respectively).

Establishment of TCb chemotherapy mouse models

Female BALB/c mice (20–25 g) were obtained from Slac Laboratory Animal Co., Ltd. (Shanghai, China) for the development of TCb chemotherapy mouse models. Briefly, the mice received weekly intraperitoneal injections of carboplatin at a dose of 50 mg/kg (Aladdin, China, Catalog No. C110682) and docetaxel at 10 mg/kg (Aladdin, Catalog No. D107320) for a duration of two weeks [15, 16]. To investigate the effects of inhibiting NETs formation on this chemotherapy model, mice received daily i.p. injections of CI-amidine at 10 mg/kg (GLPBIO, USA, Catalog No. GC35706) for seven consecutive days [17], starting after the second week of TCb drug administration. Upon completion of the model establishment, mice were euthanized, and peripheral blood was collected. The blood samples were centrifuged at 1000×g for 10 min at 4 °C, and the resulting plasma supernatant was separated. Free dsDNA in the plasma was quantified using the Quant-It PicoGreen® dsDNA Assay Kit [13, 14]. Additionally, concentrations of MPO, histone H3, vWF, and Syndecan-4 in the plasma were measured using ELISA kits (Kepeirui, Catalog Nos. H20096, H23423, H21383, H21812, respectively). The remaining plasma samples were stored at -80 °C for future use. Furthermore, the femurs and tibias of the mice were aseptically dissected and immersed in RPMI base medium (Servicebio, China, Catalog No. G4532) supplemented with 3% fetal bovine serum (FBS; Bioind, Israel, Catalog No. 04-001-1A). Bone marrow was extracted for the isolation of neutrophils, which were then used in downstream experimental procedures. All mice remained healthy at the end of the experiments.

To investigate the influence of *Slc11a1* gene expression on NETs formation and vascular injury in chemotherapy mouse models, adeno-associated viruses (AAVs) (Genechem, China) were employed to knockdown *Slc11a1* gene expression in mice. Briefly, AAV9 was used to construct short hairpin RNA (shRNA) targeting the *Slc11a1* gene. Two weeks prior to the administration of TCb therapy, each mouse received a tail vein injection of 5×10^{11} viral genomes of the AAVs encoding the shRNA, followed by the establishment of the TCb chemotherapy mouse model as previously described [18]. Upon completion of the model, mice were euthanized, and plasma samples were collected for the quantification of free dsDNA and the concentrations of MPO, histone H3, vWF, and Syndecan-4. Additionally, bone marrow neutrophils were isolated and collected for further experimentation.

Isolation and purification of neutrophils

Peripheral blood from patients and healthy volunteers and neutrophils was collected, and neutrophils were isolated and purified using a Human Peripheral Blood Neutrophil Isolation Kit (Solarbio, China, Catalog No. P9040). Briefly, human peripheral blood was layered over the separation medium provided in the kit and centrifuged at 1000×g for 30 min. The intermediate layer, containing neutrophils and a small number of erythrocytes, was collected and subjected to erythrocyte lysis with the lysis buffer included in the kit. After 30 min, the cells were centrifuged at 450×g for 10 min, washed twice with the cell wash buffer provided, and then resuspended in RPMI basal medium supplemented with 3% FBS for culturing and subsequent experimental use. For mouse bone marrow, 1 mL syringes filled with RPMI basal medium containing 3% FBS were used to flush the bone marrow cavities twice. The resulting suspension was then filtered through a 150-mesh sieve, and neutrophils were isolated and purified using a Mouse Bone Marrow Neutrophil Isolation Kit (Solarbio, Catalog No. P8550), following a similar protocol as described for the isolation and purification of neutrophils from human peripheral blood.

In vitro induction of NETs

Human neutrophils were seeded onto multi-well plates and stimulated with 100 μM carboplatin and 5 nM docetaxel. To investigate the effect of inhibiting NETs formation on neutrophils, a subset of neutrophils was

treated concurrently with chemotherapy drugs and 10 μM CI-amidine [19]. The culture supernatants containing NETs were collected, and the levels of free dsDNA were measured using the Quant-It PicoGreen® dsDNA Assay Kit. Additionally, the concentrations of MPO and histone H3 in the culture supernatants were quantified using ELISA kits.

To investigate the impact of NETs generated by neutrophils in response to chemotherapeutic drugs on vascular endothelial cells, we established a conditioned medium containing NETs using the following methodology [20, 21]: Following treatment of neutrophils with chemotherapeutic agents, the original medium which contained residual TCb agents was discarded, and the multi-well plates were washed with RPMI medium to remove any residual drugs. After removal of the supernatant, the adhered NETs at the bottom were rinsed with pre-cooled ECM complete medium (ScienCell, USA, Catalog No. 1001) to resuspend NETs in a TCb-free environment. Subsequently, the mixture was centrifuged at 1000×g for 10 min at 4 °C. The resultant cell-free supernatant containing NETs was collected as the conditioned medium for culturing vascular endothelial cells and used in subsequent experiments.

Immunofluorescence staining

Neutrophils isolated and purified from patients undergoing neoadjuvant chemotherapy for breast cancer were stained with anti-myeloperoxidase antibody (Proteintech, USA, Catalog No. 22225–1-AP, diluted 1:50) and anti-histone H3 antibody (Proteintech, Catalog No. 17168–1-AP, diluted 1:1200) [22–24]. Neutrophils derived from healthy volunteers were first treated with chemotherapeutic drugs, followed by staining with antibodies specific for MPO and histone H3. Goat anti-rabbit CoraLite® Plus 594 recombinant antibody (Proteintech, Catalog No. RGAR004, diluted 1:1000) and goat anti-rabbit CoraLite® Plus 488 recombinant antibody (Proteintech, Catalog No. RGAR002, diluted 1:1000) were employed as secondary antibodies. Nuclei were counterstained and mounted simultaneously using anti-fade mounting medium containing DAPI (Beyotime, China, Catalog No. P0131). All cellular samples were visualized, photographed, and analyzed under a fluorescence microscope (Muke, China).

Cultivation of vascular endothelial cells

Human umbilical vein endothelial cells (HUVECs) were obtained from Fuheng Biology Co., Ltd. (Shanghai, China) and maintained in ECM medium within a cell culture incubator set at 5% CO_2 and 95% air atmosphere. All cell cultures were routinely tested for Mycoplasma contamination using a Mycoplasma qPCR Detection Kit (Beyotime, China, Catalog No. C0303) and confirmed no contamination. Upon reaching 80% confluence during logarithmic phase growth, the cells were passaged, and cells from passages 4 to 6 were selected for experimentation. The cells were seeded into multi-well plates and cultured for 24 h in the previously established ECM conditioned medium containing NETs. Subsequently, these cultured HUVECs were used for subsequent experimental procedures.

Cell viability assessment

The viability of HUVECs post-treatment with NETs was evaluated using the Cell Counting Kit-8 (CCK-8) assay (GLPBIO, Catalog No. GK10001). Briefly, cells were seeded into 96-well plates and treated with the conditioned medium containing NETs. Following incubation, the cells were incubated with CCK-8 solution for 30 min, and the absorbance at 450 nm was measured using a microplate reader (Tecan, Swiss) to quantify cell viability.

Western blotting analysis

Total protein was extracted from HUVEC cells or neutrophils and separated via electrophoresis on a 10% SDS-PAGE gel. The resolved proteins were subsequently transferred onto a 0.45 μm PVDF membrane (Merck, Germany, Catalog No. IPVH00005). The membrane was then incubated overnight at 4 °C with the respective primary antibodies. Following this, the membrane was incubated for 2 h with either HRP-conjugated goat anti-rabbit IgG (Proteintech, Catalog No. SA00001-2, diluted 1:5000) or goat anti-mouse IgG (Proteintech, Catalog No. SA00001-1, diluted 1:5000). Detection of the proteins was achieved using an Enhanced Chemiluminescence (ECL) kit (Servicebio, Catalog No. G2014). The primary antibodies used in Western blotting experiments included the following: anti-GAPDH (Proteintech, Catalog No. 10494-1-AP, diluted 1:20,000), anti-VE-Cadherin (Proteintech, Catalog No. 27956-1-AP, diluted 1:2000), anti-CD31 (Proteintech, Catalog No. 11265-1-AP, diluted 1:5000), anti-Syndecan-4 (Proteintech, Catalog No. 11820-1-AP, diluted 1:1000), anti-Bax (Proteintech, Catalog No. 50599-2-Ig, diluted 1:8000), and anti-NRAMP1 (Santa Cruz, USA, Catalog No. sc-398077, diluted 1:100).

Slc11a1 knockdown in neutrophils

To knockdown the gene expression of *Slc11a1* in neutrophils, small interfering RNA (siRNA) specific to *Slc11a1* (sense strand: 5'-GGUCCAGCUAUGGUU CCAUCU-3') from Genepharma (China) was employed. In accordance with the manufacturer's instructions, the *Slc11a1*-specific siRNA was complexed with the

siRNA-mate plus transfection reagent (Genepharma, Catalog No. G04026) and then introduced into neutrophils. Following an incubation of 24 h, the neutrophils were subjected to quantitative real-time PCR (q-PCR) analysis to assess the knockdown efficiency of *Slc11a1* gene expression.

q-PCR analysis

For q-PCR analysis, neutrophils were processed using RNA extraction reagents (Servicebio, Catalog No. G3013). Total cellular RNA was extracted using chloroform-isopropanol precipitation. Following washing with 75% ethanol solution, the RNA was reverse-transcribed into cDNA using the SweScript RT I First Strand cDNA Synthesis Kit (Servicebio, Catalog No. G3330), adhering to the manufacturer's protocol. Subsequently, q-PCR was conducted using the Roche LightCycler® 96 platform with SYBR Green q-PCR Premix (Servicebio, Catalog No. G3320) following the manufacturer's protocol for preparation of the q-PCR reaction system. Each reaction was performed in a 20 μL volume, and at least three technical replicates were included for each experimental replicate. The primers used for amplification were obtained from Sangon Biotech (China) and underwent an initial denaturation step at 95 °C for 30 s, followed by 40 cycles of PCR amplification consisting of 15 s at 95 °C, 10 s at 60 °C, and 30 s at 72 °C. The fold change in target gene mRNA was normalized against GAPDH as the housekeeping gene. Melting curve analysis was performed to assess the specificity of amplification. The primer sequences employed are as follows: Human Forward *GAPDH*, 5'-GGAGCGAGATCCCTCCAAAAT-3'; Human Reverse GAPDH, 5'-GGCTGTTGTCATACTTCT CATGG-3'; Human Forward *Slc11a1*, 5'-CGTGGCGGG ATTCAAACTTCT-3'; Human Reverse *Slc11a1*, 5'-CAC CTTAGGGTAGTAGAGATGGC-3'; Mouse Forward *GAPDH*, 5'-AATGGATTGGACGCATTGGT-3'; Mouse Reverse *GAPDH*, 5'-TTTGCACTGGTACGTGTTGAT-3'; Mouse Forward *Slc11a1*, 5'-GCAGGCCCAGTTATG GCTC-3'; Mouse Reverse *Slc11a1*, 5'-CAGGCTGAA TGTACCCTGGTC-3'.

ROS analysis

The intracellular generation of ROS in neutrophils was assessed using the ROS Assay Kit (Beyotime, Catalog No. S0033). Briefly, neutrophils were incubated with DCFH-DA, which undergoes cellular esterase-mediated conversion to DCFH and subsequent oxidation by ROS into the fluorescent product DCF. Following three washes with PBS to remove excess reagent, fluorescence emission from the cells was visualized and photographed with a fluorescence microscope for subsequent analysis.

Determination of intracellular ferrous ions

Fluorescent staining of ferrous ions within neutrophils was conducted using an intracellular ferrous ion-specific fluorescent probe (Dojindo, Japan, Catalog No. F374) [25]. After washing of neutrophils thoroughly three times with serum-free culture medium, the cells were incubated with the ferrous ion probe, which binds to intracellular ferrous ions, resulting in the generation of fluorescence. The fluorescence intensity, indicative of ferrous ion content, was then visualized and captured using a fluorescence microscope and flow cytometry (Thermo Fisher Scientific, USA) for analysis.

RNA sequencing

Total RNA was extracted using Trizol reagent (Invitrogen, USA, Catalog No. 15596026CN), and the purity, concentration, and integrity of the RNA samples were evaluated prior to further analysis with an Agilent 2100 bioanalyzer (Agilent, USA). Library preparations were sequenced on the Illumina platform at Novogene (China), and raw reads were generated. Subsequently, raw reads were filtered to remove adapters, poly-N sequences, and low-quality reads. Clean reads were then mapped to the mouse reference genome sequence with the HISAT2 tool. Gene expression levels were estimated by calculating fragments per kilobase of transcript per million mapped fragments. Differential gene expression analysis between groups was performed with DESeq2, with genes exhibiting P values < 0.05 designated as differentially expressed genes (DEGs). Subsequently, enrichment analysis of DEGs was conducted with clusterProfiler software. Reactome enrichment analysis and heatmaps were generated on the NovoMagic platform (https://magic.novogene.com/customer/main#). Raw data is available upon reasonable request from the corresponding author.

Statistical analysis

Data is presented as mean ± standard deviation (SD). Prior to parametric tests, all datasets were validated for normality using the Shapiro–Wilk test and homogeneity of variances using Levene's test. For comparative analysis between two groups, an unpaired two-tailed t-test was used. For multiple comparisons involving three or more groups, a one-way analysis of variance (ANOVA) was conducted. For all ANOVA analyses, post hoc pairwise comparisons were performed using Tukey's HSD test to determine specific group differences when a significant overall effect was detected. All datasets met the assumptions of normality ($p > 0.05$) and homogeneity of variances ($p > 0.05$), supporting the use of parametric tests. A P value < 0.05 was considered statistically significant. Graphical representation and statistical

analyses were performed with GraphPad Prism version 8.0 software (GraphPad Software, Inc., USA).

Results

TCb Chemotherapy Promotes NETs Formation in Breast Cancer Patients and Mouse Models

To investigate whether neoadjuvant chemotherapy regimens for breast cancer can stimulate the formation of NETs in patients, we measured the levels of NETs dsDNA, MPO, and Histone H3 in the plasma of patients undergoing neoadjuvant chemotherapy for breast cancer, as well as in control patients. The baseline characteristics of patients are shown in Supplementary Table 1. Compared to the control group, patients receiving TCb neoadjuvant chemotherapy exhibited elevated levels of NETs dsDNA in the plasma, accompanied by increased levels of MPO and Histone H3. However, no significant differences in plasma NETs dsDNA, MPO, and Histone H3 were observed between patients undergoing EC-T or EC-T-HP neoadjuvant chemotherapy and the control group (Fig. 1A, B). These findings suggest that patients treated with the TCb neoadjuvant chemotherapy for breast cancer experience an increase in NETs formation. To validate these results, we isolated neutrophils from control patients and breast cancer patients treated with the TCb chemotherapy regimen and performed immunofluorescence staining. We found that MPO and Histone H3 showed more pronounced co-expression in neutrophils from TCb-treated patients compared to the control group (Fig. 1C, D). This also provides evidence that NETs levels are significantly elevated in TCb-treated patients.

To further evaluate whether TCb neoadjuvant chemotherapy drugs lead to an increase in NETs formation in vivo, we applied TCb chemotherapy agents in mice to construct TCb chemotherapy mouse models. In the TCb chemotherapy mouse models, a significant elevation was observed in the levels of NETs dsDNA, MPO, and Histone H3 in the plasma compared to the control group (Fig. 1E, F). These results also indicate that TCb chemotherapy drugs promote the formation of NETs in mice.

NETs Formation is Associated with the Augmentation of Endothelial Injury Markers in Breast Cancer Patients

To evaluate the impact of NETs formation on vascular endothelial injury, we measured the levels of Syndecan-4 and vWF in the plasma of breast cancer patients undergoing neoadjuvant chemotherapy. Our analysis revealed a significant upregulation of Syndecan-4 and vWF levels in the plasma of patients treated with the TCb chemotherapy regimen compared to the control group. Conversely, patients receiving EC-T and EC-T-HP chemotherapy regimens did not exhibit significant alterations in the levels of these vascular endothelial injury markers, as compared to the control cohort (Fig. 2A). Furthermore, a correlation analysis between the plasma levels of Syndecan-4, vWF, and NETs dsDNA was performed, demonstrating a significant association between the two endothelial injury markers and plasma NETs dsDNA levels (Fig. 2B). These findings suggest a close correlation between NETs formation induced by the TCb neoadjuvant chemotherapy regimen in breast cancer patients and the augmentation of vascular endothelial injury markers.

TCb Chemotherapeutic Agent induced NETs Formation in Neutrophils and NETs-Mediated Vascular Endothelial Cell Damage In Vitro

To further investigate the effects of chemotherapeutic drugs on NETs formation in neutrophils, we extracted neutrophils from healthy volunteers and induced them with TCb chemotherapeutic drug in vitro (Fig. 3A). Our results demonstrated that, following an eight-hour induction with TCb, the concentration of NET dsDNA in the cell culture supernatant significantly increased compared to the control group (Fig. 3B). At this time point, we also measured the levels of MPO and Histone H3 in the cell culture supernatant, which showed significant elevations compared to the control (Fig. 3C). Additionally, we performed immunofluorescence staining on neutrophils induced with TCb chemotherapeutic agents in vitro. Notably, neutrophils induced with TCb exhibited a more pronounced co-expression of MPO and Histone H3 compared to the control group (Fig. 3D, E). Collectively, these findings indicate that TCb chemotherapeutic drug can induce NETs production by neutrophils in vitro.

To investigate whether NETs generated by neutrophils in response to the TCb chemotherapeutic agent are associated with damage to vascular endothelial cells in vitro, we devised a conditioned medium enriched with NETs following TCb treatment of neutrophils and used this medium for the in vitro culture of HUVECs (Fig. 3A). Our findings revealed a marked decrease in the cellular viability of HUVECs cultured in the NETs-containing conditioned medium compared to the control group (Fig. 3F). Additionally, we examined the protein levels of endothelial markers, including VE-cadherin, CD31, and Syndecan-4, along with the apoptotic marker Bax, in vascular endothelial cells. Notably, treatment with the NET-enriched conditioned medium led to a pronounced decrease in the protein levels of endothelial markers, accompanied by a significant elevation in the protein level of Bax (Fig. 3G, H). To compare these effects with the direct toxicity of TCb chemotherapeutic agents, we also

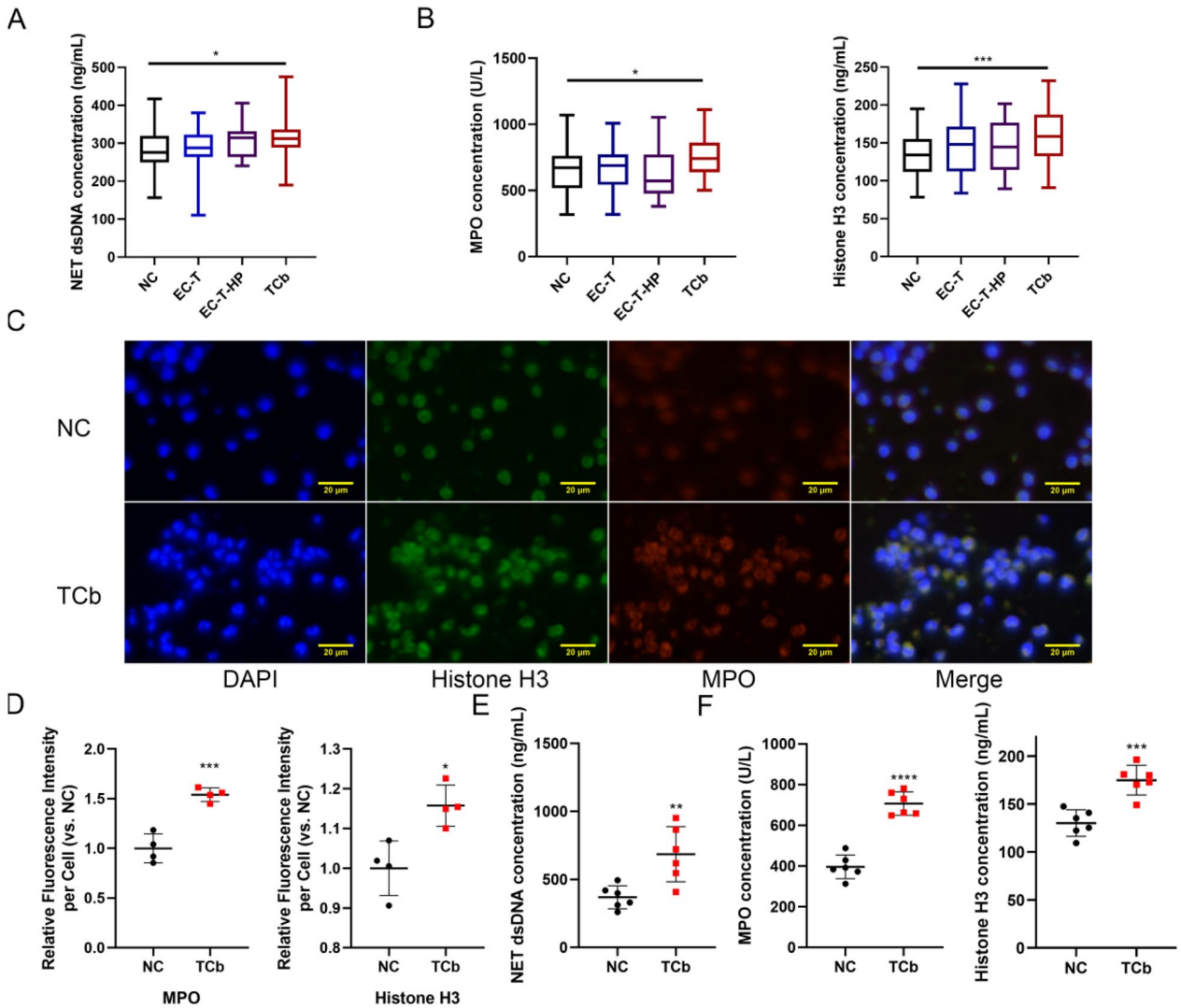

Fig. 1 TCb Enhances Neutrophil Extracellular Traps (NETs) Formation in Neoadjuvant Chemotherapy Patients and Animal Models. **A** Plasma dsDNA concentrations in normal control breast cancer patients, and those undergoing EC-T, EC-T-HP and TCb neoadjuvant chemotherapy. Plasma dsDNA levels were significantly elevated in TCb-treated patients compared to controls. NC (n = 50), EC-T (n = 50), EC-T-HP (n = 19), TCb (n = 45), **B** plasma Myeloperoxidas (MPO) and histone H3 concentrations in patients showed significant increases in TCb-treated patients compared to controls, **C**, **D** immunofluorescence staining showed more pronounced co-expression of MPO and histone H3 in neutrophils from TCb-treated patients than controls, **E** plasma dsDNA concentrations in mice from TCb chemotherapy models and controls. Plasma dsDNA was significantly elevated in TCb model mice compared to controls (n = 6), **F** plasma MPO and histone H3 concentrations in mouse models showed significant increases in TCb models compared to controls. * $P < 0.05$, ** $P < 0.01$, *** $P < 0.001$, **** $P < 0.0001$

treated HUVECs with TCb alone. While TCb treatment slightly reduced HUVECs viability, the inhibition was less pronounced than that induced by NETs (Supplementary Fig. 1A). Furthermore, TCb treatment caused a reduction in the protein levels of endothelial markers (VE-cadherin, CD31, Syndecan-4) and an increase in the apoptotic marker Bax (Supplementary Fig. 1B-C). However, these effects were less pronounced compared to the changes induced by NETs. Collectively, these results demonstrate that NETs generated by neutrophils in response to TCb chemotherapeutic agent in vitro contribute to reduced vascular endothelial cell viability, increased apoptosis, and ultimately, damage to vascular endothelial cells.

CI-amidine mitigated the Elevation of NETs and the Subsequent Vascular Endothelial Injury in TCb Mouse Chemotherapy Models

To further investigate the implications of altered NETs levels on vascular endothelial injury in mice, we employed the PAD4 inhibitor CI-amidine, targeting

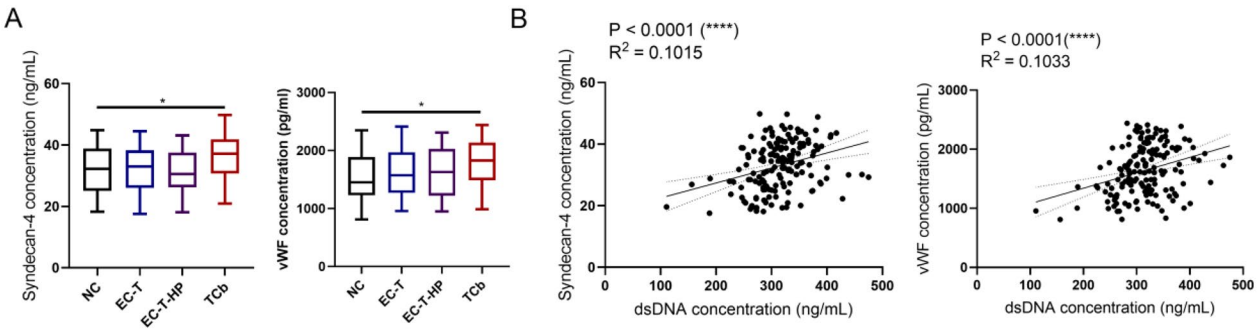

Fig. 2 NETs Formation is Associated with Vascular Endothelial Injury in Breast Cancer Patients Undergoing Neoadjuvant Chemotherapy. **A** Concentrations of Syndecan-4 and vWF were measured in breast cancer patients. Patients undergoing TCb neoadjuvant chemotherapy exhibited significantly elevated levels of Syndecan-4 and vWF compared to controls. NC (n = 50), EC-T (n = 50), EC-T-HP (n = 19), TCb (n = 45), **B** a positive correlation was observed between plasma concentrations of Syndecan-4/vWF and dsDNA in breast cancer patients undergoing neoadjuvant chemotherapy. * $P < 0.05$, **** $P < 0.0001$

NETs formation within TCb chemotherapy mouse models. PAD4 is an enzyme crucial for NETs formation, mediating histone citrullination during NETs formation [26, 27]. To validate CI-amidine's inhibitory effect on NETs production, we treated neutrophils subjected to in vitro TCb chemotherapy with CI-amidine. Notably, the levels of NETs dsDNA, MPO and histone H3 in the cell culture supernatants were significantly reduced following CI-amidine administration compared to the TCb-only treatment group (Supplementary Fig. 2A, B). Furthermore, immunofluorescence assays also revealed a marked attenuation in the co-expression of MPO and histone H3 in mice treated with CI-amidine in addition to TCb chemotherapy, compared to TCb alone (Supplementary Fig. 2C, D). Subsequently, we extended this treatment paradigm to the TCb chemotherapy mouse models (Fig. 4A). We observed a pronounced decrease in plasma concentrations of NETs dsDNA, MPO, and histone H3 in mice that received CI-amidine in conjunction with TCb chemotherapy, as opposed to TCb chemotherapy alone (Fig. 4B, C). These findings collectively indicate that CI-amidine is effective in reducing NETs formation by neutrophils at both cellular and animal levels. Building upon these observations, we assessed plasma levels of the vascular endothelial injury markers Syndecan-4 and vWF in mouse models. Notably, TCb chemotherapy in mice significantly elevated plasma levels of Syndecan-4 and vWF compared to controls. Importantly, the augmentation of these injury markers was partially reversed upon treatment with CI-amidine (Fig. 4D). Our results suggest that the increased NETs generation induced by TCb chemotherapy in mouse models contributes to vascular endothelial injury.

Upregulation of *Slc11a1* in Neutrophils Induced by TCb Chemotherapy Agent Leads to Increased Intracellular Ferrous Ion Content, ROS Generation and NETs Formation

To elucidate the mechanisms underlying the increased NETs formation induced by the TCb chemotherapeutic agent, we conducted RNA sequencing analysis on neutrophils isolated from both TCb-treated mice and the untreated controls. Our results demonstrated an upregulation of 1,284 genes and downregulation of 1,011 genes in TCb-treated mice compared to controls (Fig. 5A). Subsequently, Reactome functional enrichment analysis and Gene Set Enrichment Analysis (GSEA) were performed on these differentially expressed genes, revealing a prominent upregulation of the ROS, RNS Production in Phagocyte signaling pathway within the TCb-treated mouse model (NOM $p = 0.000$, FDR

(See figure on next page.)

Fig. 3 Induction of NETs Following TCb Stimulation, Demonstrating NETs-Mediated Damage in Human Umbilical Vein Endothelial Cells (HUVECs). **A** Schematic representation of the experimental setup, illustrating the in vitro application of the TCb chemotherapeutic agent to induce NETs formation in neutrophils and generate conditioned media containing NETs for treating HUVECs, **B** neutrophils extracted from healthy volunteers were treated with TCb for 4, 8, and 24 h in vitro. An increase in NETs dsDNA concentration in the cell culture supernatant was observed starting 8 h post-treatment, **C** After 8 h of TCb treatment, significant elevations in MPO and histone H3 concentrations were observed in the cell culture supernatant of the TCb-treated group compared to the untreated control, **D**, **E** immunofluorescence staining revealed a more pronounced co-expression of MPO and histone H3 in TCb-treated human neutrophils compared to untreated controls, **F** cell viability of HUVECs treated with TCb-induced NETs was assessed using the CCK-8 assay, revealing a significant decrease compared to untreated controls, **G**, **H** western blot analysis revealed significant downregulation of VE-cadherin, CD31, and Syndecan-4, and upregulation of Bax in HUVECs treated with TCb-induced NETs, indicating endothelial cell injury and apoptosis. * $P < 0.05$, ** $P < 0.01$, *** $P < 0.001$, **** $P < 0.0001$

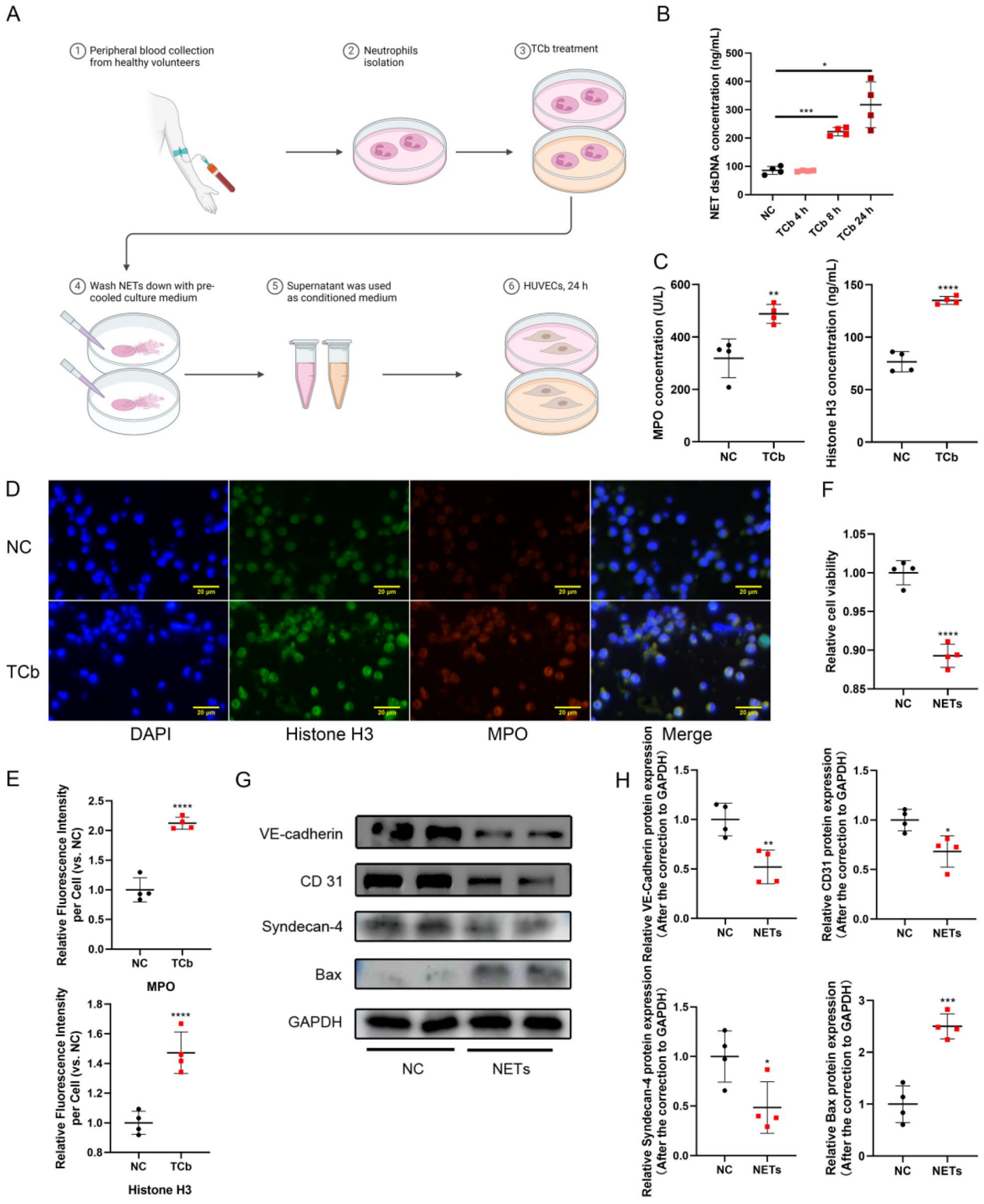

Fig. 3 (See legend on previous page.)

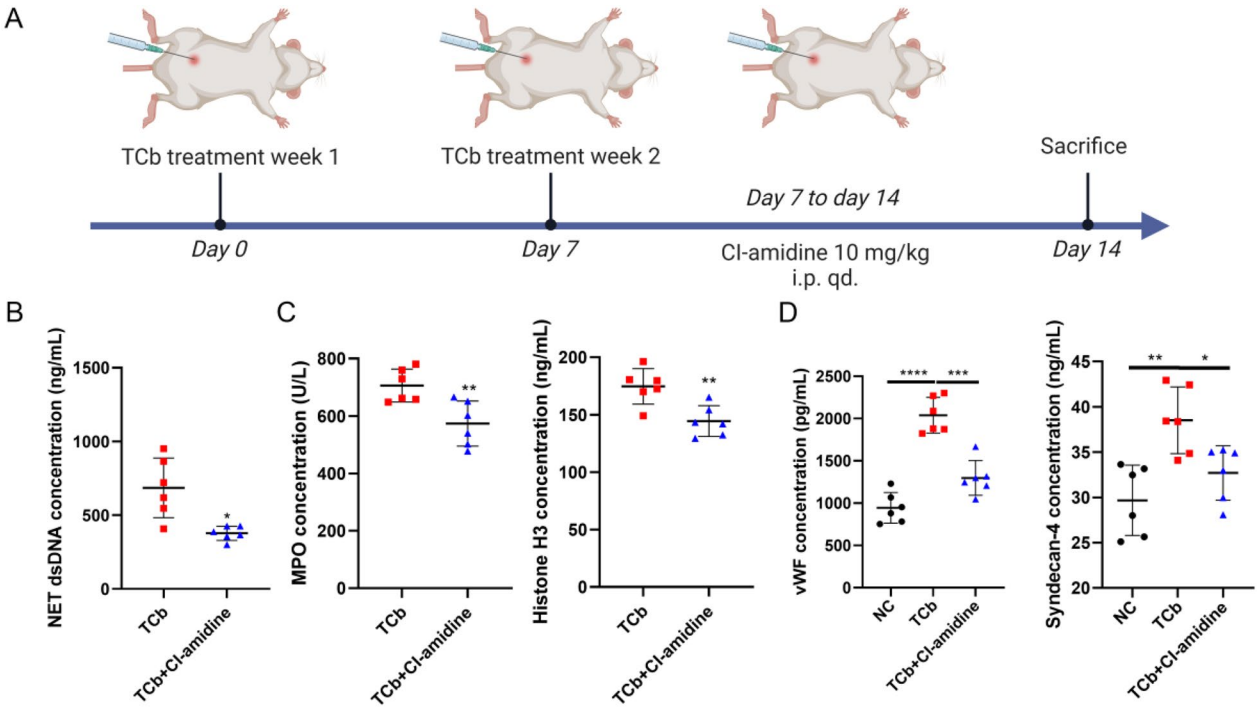

Fig. 4 Reversal of Vascular Endothelial Injury Markers Induced by NETs Formation in TCb Mouse Models. **A** Schematic representation of the mouse models used for TCb chemotherapy and CI-amidine intervention, **B** administration of CI-amidine to TCb mouse models reversed the elevated plasma dsDNA concentrations observed in TCb-treated mice (n = 6), **C** plasma levels of MPO and histone H3 in mouse models showed that CI-amidine mitigated increases induced by TCb chemotherapy, **D** plasma concentrations of vWF and Syndecan-4, significantly upregulated in TCb-treated mice compared to controls, were reversed by CI-amidine intervention. * $P < 0.05$, ** $P < 0.01$, *** $P < 0.001$, **** $P < 0.0001$

q = 0.003, FWER $p = 0.008$) (Fig. 5B, C), which was prioritized for further investigation due to its established role in NETs formation. This finding suggests enhanced production of ROS and RNS in neutrophils from TCb-treated mice. To further investigate, we compared the expression profiles of all genes implicated in the signaling pathway between TCb-treated and control mice, represented in a heatmap. Notably, a substantial upregulation of *Slc11a1*, a gene closely associated with the transport of divalent metal ions [28], including Fe^{2+}, Zn^{2+}, $Co^{2+}$and Mn^{2+}, across the phagocyte membrane [29, 30], was observed in TCb-treated mice (Fig. 5D). Despite ranking second in differential expression within this pathway (following *Cybb*, a canonical NADPH oxidase subunit), *Slc11a1* was selected for mechanistic studies due to its novel role in phagocyte iron transport—a potential driver of ROS generation distinct from canonical DNA damage pathways. Specifically, the *Slc11a1* gene encodes the NRAMP1 protein, which localizes to the phagocyte membrane and facilitates the influx of divalent metal ions from the extracellular space into the cell [31]. These metal ions, particularly Fe^{2+}, contribute to heightened ROS production within phagocytes [32], thereby facilitating

(See figure on next page.)

Fig. 5 Differential *Slc11a1* Expression Leads to Enhanced Reactive Oxygen Species (ROS), Ferrous Ion and NETs Content. **A** RNA sequencing of neutrophils isolated from mouse chemotherapy models identified 1,284 upregulated and 1,011 downregulated genes (n = 3), **B**, **C** reactome and GSEA analyses characterized the functional significance of the differentially expressed genes (DEGs). Enrichment analysis highlighted prominent clustering of differentially expressed genes within the ROS, RNS Production in Phagocyte signaling pathway, **D** a gene heatmap of the ROS, RNS Production in Phagocyte pathway illustrates significant upregulation of *Slc11a1* gene expression in the TCb chemotherapy model compared to controls, **E** q-PCR analysis revealed a significant upregulation of *Slc11a1* mRNA in human neutrophils treated with TCb chemotherapy in vitro, **F**, **G** western blot assays showed a marked increase in NRAMP1 protein expression in TCb-treated human neutrophils compared to controls, **H**–**J** a significant elevation in ferrous ion content was detected in TCb-treated human neutrophils using the FerroOrange probe, **K**, **L** measurement of ROS levels using a ROS detection kit showed a pronounced increase in ROS production in human neutrophils exposed to TCb chemotherapy. * $P < 0.05$, ** $P < 0.01$, *** $P < 0.001$, **** $P < 0.0001$

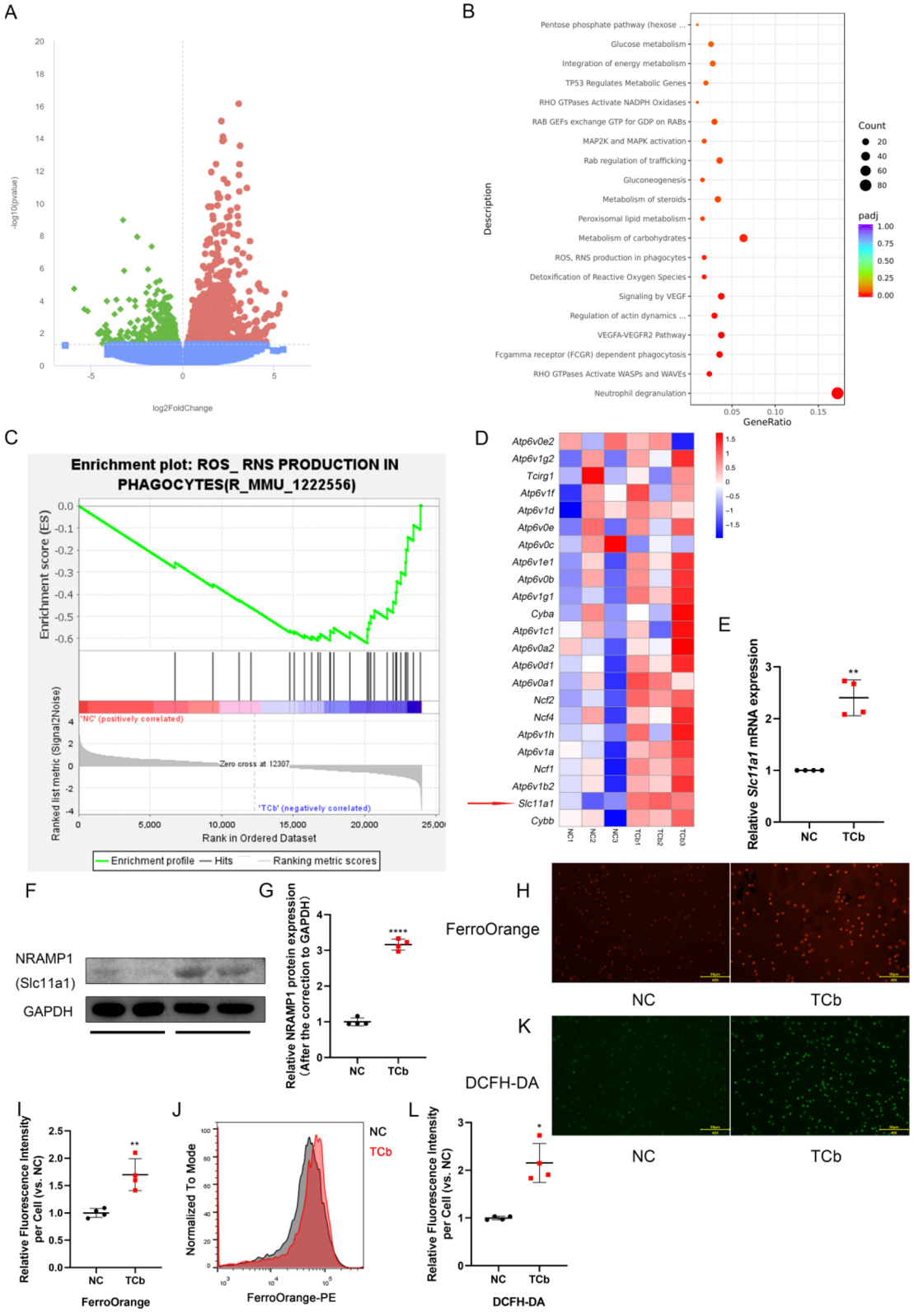

Fig. 5 (See legend on previous page.)

NETs formation. Based on these findings, we hypothesize that TCb chemotherapy promotes an increase in *Slc11a1* expression in neutrophils, leading to elevated levels of NRAMP1 protein. This, in turn, enhances the influx of divalent metal ions, predominantly Fe^{2+}, into the cell, stimulating a surge in intracellular ROS generation. Ultimately, this cascade of events culminates in the augmentation of NETs production.

To validate the findings from RNA sequencing, we treated neutrophils cultured in vitro with the TCb chemotherapeutic agent and examined the intracellular *Slc11a1*expression. Our results demonstrated a significant upregulation of *Slc11a1* mRNA expression in neutrophils treated with TCb compared to untreated controls (Fig. 5E). Subsequently, we quantified the intracellular NRAMP1 protein content via Western blot analysis, revealing a marked increase in NRAMP1 protein expression in TCb-treated neutrophils (Fig. 5F, G). Furthermore, we assessed the intracellular Fe^{2+} content in neutrophils using a ferrous ion probe. Notably, neutrophils treated with TCb exhibited a significantly elevated Fe^{2+} content compared to the control group (Fig. 5H, J). Lastly, we used an ROS detection kit to measure ROS levels within neutrophils. Consistent with our other observations, TCb-treated neutrophils displayed a notable increase in ROS production compared to untreated controls (Fig. 5K, L). Collectively, these findings indicate that the TCb chemotherapeutic agent can induce increased expression of the *Slc11a1* gene in neutrophils, leading to elevated NRAMP1 protein levels, subsequently augmenting intracellular Fe^{2+} content and enhancing ROS generation.

Knockdown of *Slc11a1* In Vitro Reverses TCb-Induced Elevated Intracellular Ferrous Ion Content, ROS Generation and NETs Formation

To further validate the role of the *Slc11a1* gene in NETs formation of neutrophils in vitro, we employed siRNA to knockdown *Slc11a1* expression. Quantification of *Slc11a1* mRNA expression revealed significant upregulation in neutrophils treated with the TCb chemotherapeutic agent compared to non-targeting siRNA controls. Knockdown of *Slc11a1* led to a marked reduction in expression levels, whether with TCb or non-TCb treatment (Fig. 6A). Correspondingly, Western blot analysis of NRAMP1 protein across different treatment groups mirrored these mRNA findings. TCb-treated neutrophils transfected with non-targeting siRNA exhibited increased NRAMP1 protein levels. Conversely, NRAMP1 protein levels were significantly decreased in neutrophils with *Slc11a1* knocked down (Fig. 6B, C). Additionally, we used ferrous ion probes and ROS detection kits to assess intracellular ferrous iron content and ROS production, respectively. As expected, TCb treatment elevated Fe^{2+} content and ROS levels in neutrophils transfected with non-targeting siRNA. Knockdown of *Slc11a1* reversed these TCb-induced increases in Fe^{2+} and ROS (Fig. 6D–H). Finally, analysis of culture supernatants revealed that TCb treatment upregulated levels of NETs dsDNA, MPO, and histone H3. Notably, the upregulation of these markers was abrogated by *Slc11a1* knockdown (Fig. 6I–J). These findings collectively suggest that interference with *Slc11a1* in neutrophils reverses TCb-mediated increases in Fe^{2+} content, ROS levels, and subsequently NETs formation.

Slc11a1 Knockdown in Vivo Attenuates NETs formation and Vascular Endothelial Injury Markers in mouse Chemotherapy Models

To further validate the impact of *Slc11a1* expression on mouse chemotherapy models, we generated *Slc11a1*-knockdown mice via tail vein injection of AAVs, and subsequently established TCb chemotherapy models in these mice (Fig. 7A). q-PCR analysis of *Slc11a1* mRNA levels in neutrophils from TCb model mice revealed a significant upregulation of *Slc11a1* mRNA compared to neutrophils from mice treated with empty AAVs, while *Slc11a1*-knockdown mice exhibited significantly reduced *Slc11a1* mRNA expression compared to the empty AAVs group (Fig. 7B). Subsequently, we used ferrous ion probes and ROS detection kits to quantify the intracellular Fe^{2+}

(See figure on next page.)

Fig. 6 *Slc11a1* Knockdown Reduces ROS, Ferrous Ion Contents and NETs Production in Human Neutrophils In Vitro. **A** Human neutrophils were treated with the TCb chemotherapeutic agent or transfected with *Slc11a1* small interfering RNA (siRNA). *Slc11a1* mRNA levels were measured by q-PCR. TCb treatment significantly increased *Slc11a1* mRNA expression, which was reversed upon knockdown of *Slc11a1*, **B**, **C** western blot analysis showed that TCb treatment significantly elevated NRAMP1 protein levels in human neutrophils, which was reversed by *Slc11a1* knockdown, **D**–**F** intracellular ferrous ion levels, measured using the FerroOrange probe in human neutrophils, showed a significant increase in TCb-treated groups, attenuated by *Slc11a1* knockdown, **G**, **H** ROS levels in TCb-treated human neutrophils demonstrated a marked elevation compared to controls, which was reversed by *Slc11a1* knockdown, **I** quantification of dsDNA in cell culture supernatants showed a significant increase in TCb-treated human neutrophils, which was significantly reversed by *Slc11a1* knockdown, **J** MPO and histone H3 concentrations in the culture supernatants of TCb-treated human neutrophils were elevated but reversed by *Slc11a1* knockdown. * $P < 0.05$, ** $P < 0.01$, *** $P < 0.001$, **** $P < 0.0001$

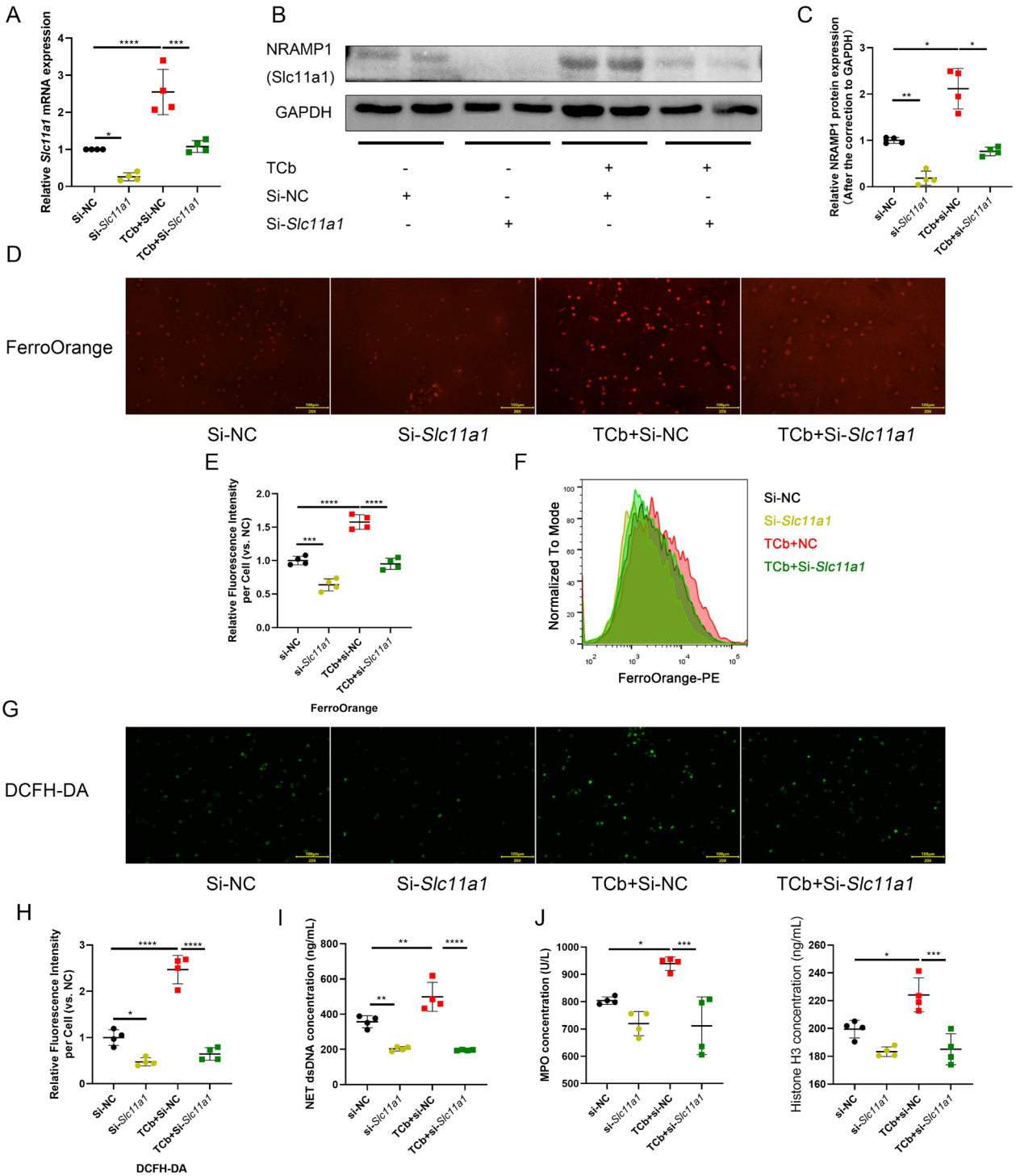

Fig. 6 (See legend on previous page.)

content and ROS generation in neutrophils from each group. Notably, TCb-treated mice exhibited significantly elevated Fe^{2+} and ROS levels in their neutrophils compared to controls. However, *Slc11a1* knockdown significantly reversed the TCb-induced increases in both Fe^{2+} content and ROS generation in neutrophils (Fig. 7C–G). Plasma analysis further revealed that TCb treatment elevated the levels of NETs dsDNA, MPO, and histone H3, and these elevations were also mitigated upon *Slc11a1* knockdown (Fig. 7H, I). Additionally,

we assessed plasma levels of vWF and Syndecan-4, found to be elevated in TCb-treated mice. *Slc11a1* knockdown significantly reversed the increases in both vWF and Syndecan-4 levels (Fig. 7J). Collectively, these findings underscore that *Slc11a1* knockdown in TCb chemotherapy models significantly reduces Fe^{2+} and ROS content within neutrophils, thereby inhibiting the TCb-induced augmentation of NETs formation and effectively reversing associated endothelial damage.

Discussion

In this study, we demonstrated that TCb neoadjuvant chemotherapy for breast cancer promotes NETs formation, which is closely linked to vascular endothelial injury in patients, HUVECs and mouse models. The use of PAD4 inhibitor CI-amidine to block NETs formation significantly mitigated the elevation of vascular endothelial injury markers in TCb chemotherapy mouse models. Additionally, RNA sequencing analysis identified *Slc11a1* as a key gene potentially involved in TCb-induced NETs formation. We verified that TCb chemotherapy upregulates *Slc11a1* expression in neutrophils, leading to increased intracellular ferrous iron content and ROS levels, thereby facilitating NETs formation. Importantly, *Slc11a1* knockdown in neutrophils and chemotherapy mouse models reversed these effects, reducing NETs production and mitigating the upregulation of vascular endothelial injury markers. Collectively, these findings underscore a novel role for *Slc11a1* in modulating intracellular ferrous iron levels and ROS generation, crucial for TCb-induced NETs formation and subsequent endothelial damage.

Neoadjuvant chemotherapy represents a pivotal component of the individualized multimodal approach to breast cancer management [33, 34]. However, its detrimental effects, notably on vascular endothelial function, have been extensively documented in various researches. A seminal study published in the Journal of Clinical Investigation in 2022 highlighted significant impairment of vascular function, particularly endothelial-dependent, nitric oxide-mediated vascular injury, in breast cancer patients undergoing neoadjuvant chemotherapy regimens comprising docetaxel, doxorubicin, and cyclophosphamide [16]. Additionally, neoadjuvant chemotherapy was found to exacerbate endothelial damage and enhance glycocalyx degradation, leading to diminished glycocalyx thickness [35, 36]. Our investigation demonstrated an upregulation of vascular endothelial injury markers vWF and Syndecan-4 in TCb-treated breast cancer patients. vWF is a glycoprotein synthesized and secreted by vascular endothelial cells and megakaryocytes, playing pivotal roles in the vascular system [37]. Syndecan-4, a critical constituent of the endothelial glycocalyx [38], shows elevated in plasma levels indicative of glycocalyx shedding due to endothelial damage [39], thus emerging as an indicator of vascular injury [40]. Notably, endothelial injury in breast cancer patients predisposes them to a hypercoagulable state, precipitating adverse outcomes such as thromboembolism [41]. Therefore, the mechanistic insights elucidated in our study have significant potential to guide the prevention and management of perioperative hypercoagulability and related complications in breast cancer patients undergoing neoadjuvant chemotherapy.

Neutrophils and their orchestrated nonspecific immunity represent the second line of defense in the human body [42]. As crucial effector cells in the innate immune system, neutrophils can be activated by endogenous or exogenous stimuli, leading to oxidative stress and ROS generation [43]. Cytotoxic chemotherapy agents, such as TCb [44], elicit oxidative stress and ROS production in neutrophils. Studies have shown that doxorubicin induces cardiotoxicity through oxidative stress activation within the innate immune system [45]. Moreover, an investigation of TCb chemotherapy agents revealed that carboplatin and paclitaxel induce widespread oxidative stress in peritoneal cells, crucially contributing to their activation and senescence [46]. However, it is critical to note that not all chemotherapeutic agents promote

(See figure on next page.)

Fig. 7 *Slc11a1* Knockdown in Mouse Models Leads to Reduced ROS, Ferrous Ions and NETs in Neutrophils. **A** Schematic representation of generating *Slc11a1* knockdown mice using AAV constructs and constructing a TCb chemotherapy mouse model, **B** q-PCR analysis of *Slc11a1* mRNA expression in neutrophils from mouse models. Significant increases in *Slc11a1* mRNA expression in neutrophils from TCb-treated mice were reversed in *Slc11a1*-knockdown TCb-treated mice, **C**–**E** detection of ferrous ion levels in neutrophils from mouse models. Elevated ferrous ion content in neutrophils from TCb-treated mice was notably reversed in *Slc11a1*-knockdown mice, **F**, **G** measurement of ROS levels in neutrophils from mouse models. Elevated ROS levels in neutrophils from TCb-treated mice were significantly mitigated in *Slc11a1*-knockdown mice, **H** quantification of dsDNA in plasma from mouse models. Increased plasma dsDNA concentrations in TCb-treated mice were significantly attenuated in *Slc11a1*-knockdown mice, **I** analysis of MPO and histone H3 levels in plasma from mouse models. Elevated concentrations of MPO and histone H3 in plasma from TCb-treated mice were significantly reversed in *Slc11a1*-knockdown mice, **J** assessment of vWF and Syndecan-4 levels in plasma from mouse models. Increased plasma concentrations of vWF and Syndecn-4 in TCb-treated mice were significantly diminished in *Slc11a1*-knockdown mice. * $P < 0.05$, ** $P < 0.01$, *** $P < 0.001$, **** $P < 0.0001$

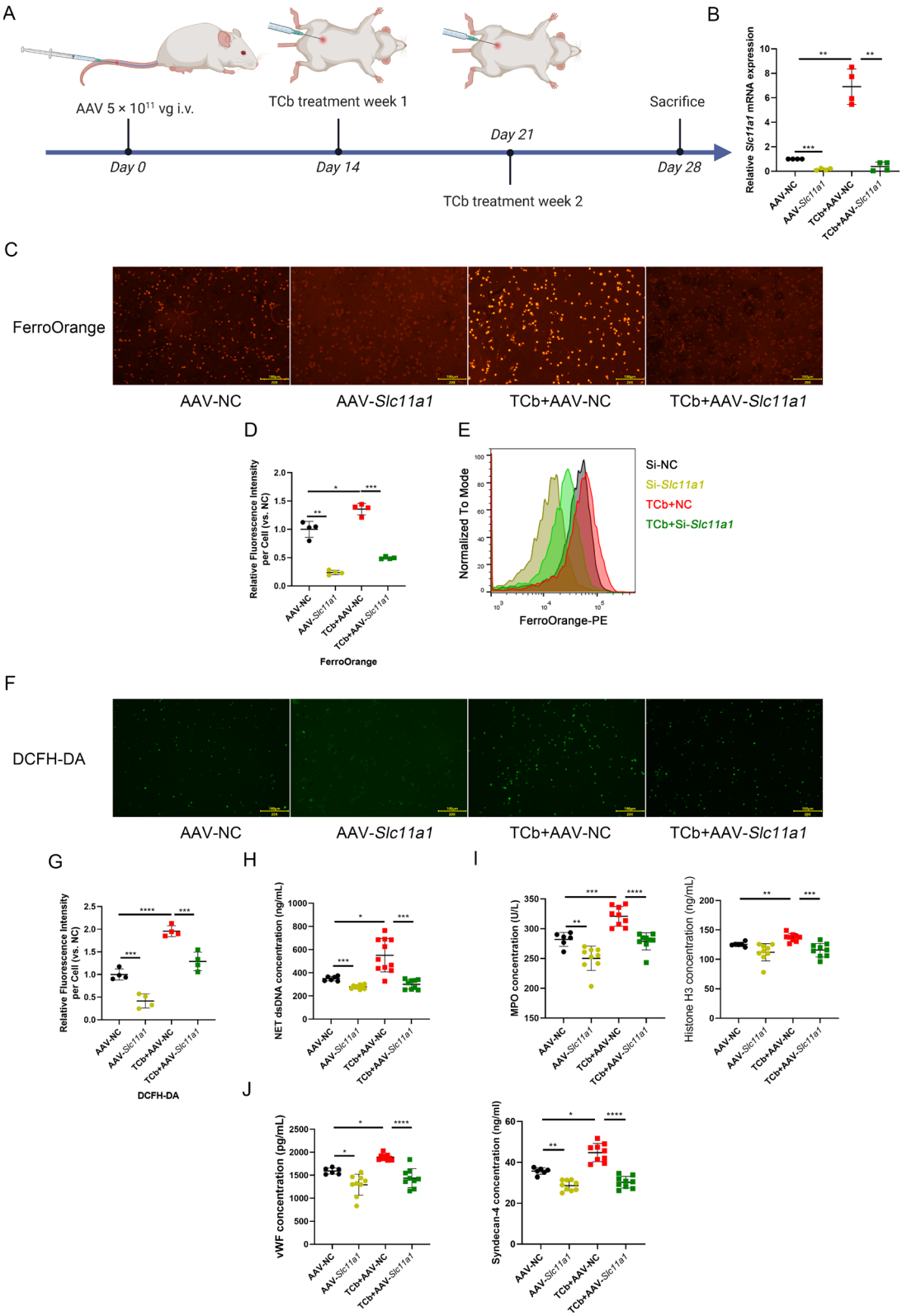

Fig. 7 (See legend on previous page.)

NETs formation in neutrophils. In our clinical cohort, patients receiving EC-T-based neoadjuvant chemotherapy showed no significant elevation in plasma NETs levels. This observation aligns with prior studies demonstrating that anthracyclines (e.g., epirubicin, doxorubicin) suppress both NADPH oxidase-dependent and -independent NETs formation in human neutrophils in vitro. The intercalating properties of anthracyclines may disrupt transcriptional initiation, thereby inhibiting NETs formation [47]. These findings highlight the heterogeneity of chemotherapy-induced NETs formation mechanisms. Future studies should systematically compare NETs induction across drug classes to delineate drug-specific effects.

The relationship between ROS and NETs formation is well-established, as exemplified by studies demonstrating NETs formation via the ROS/MAPK/PAD4 axis [48] and ROS generation in the mouse brain [49]. Mitochondria, as key regulators of intracellular ROS and RNS production, have also been extensively implicated in NETs formation. For instance, mitochondrial respiration not only promotes NETs formation but is reciprocally amplified by NETs through enhanced metabolic coupling [50], potentially modulated by chemotherapeutic agents. Additionally, mitochondrial damage may trigger NETs formation by releasing mitochondrial DNA (mtDNA), which activates neutrophil inflammatory pathways [51]. In our study, RNA sequencing of mouse neutrophils, along with subsequent in vivo and in vitro validation experiments, highlighted a significant enrichment of DEGs in the ROS, RNS Production in Phagocyte signaling pathway. Our RNA sequencing data, combined with prior studies, suggest a potential link between ROS production, mitochondrial activity, and chemotherapy-induced NETs formation. NETs also inflict self-damage, notably in organs such as the lungs, liver, and kidneys [52–54], and contribute to vascular endothelial injury. Previous studies have extensively reported NETs-mediated vascular endothelial damage, with evidence suggesting NETs induce lung microvascular endothelial pyroptosis via NLRP3 inflammasome activation [55] and promote thrombosis leading to neutrophil cytoplasmic antibody-associated vasculitis [56]. Consistent with these findings, our study observed alterations in vascular endothelial markers associated with NETs production. Additionally, Our findings revealed that the PAD4 inhibitior CI-amidine effectively suppresses NETs formation and mitigates vascular endothelial injuries. In summary, our study linked the TCb neoadjuvant chemotherapy to NETs formation induced by ROS and elucidated their relationship with vascular endothelial injury.

The solute carrier transporter family, regarded as the metabolic gatekeepers of cells, oversees the transport of nutrients and metabolites within cellular compartments [57]. Among them, *Slc11a1* stands out as a crucial gene intimately linked to intracellular metal ion transport [58]. *Slc11a1*, predominantly expressed in phagocytes such as neutrophils and macrophages [59], facilitates metal ion influx and stimulate intracellular ROS generation via the Fenton reaction [60–62]. Prior studies have demonstrated that *Slc11a1* upregulation promotes ROS production in phagocytes [63]. In our investigation, we corroborate these findings by observing elevated ferrous ion concentrations and consequent ROS formation in neutrophils with TCb chemotherapy-induced *Slc11a1* upregulation. Previous studies have provided limited insight into the relationship between *Slc11a1* and extracellular traps. A genetic study in hybrid chickens suggested a correlation between the production of heterophil (analogous to mammalian neutrophils) extracellular traps and *Slc11a1* expression in chicken heterophils [64], supporting our research endeavors. However, the relationship between *Slc11a1* upregulation and mammalian NETs formation remains largely unexplored. Our study revealed that TCb chemotherapy-induced *Slc11a1* upregulation leads to augmented ROS production, ultimately triggering NETs formation. This finding offers a novel explanatory pathway for NETs formation associated with chemotherapy.

In neutrophils, differential expression of *Slc11a1* modulates their functions, ultimately contributing to cellular and tissue damage. For instance, in patients with nontuberculous mycobacterial infections, transcriptome analyses have implicated the *Slc11a1* gene in promoting neutrophil-induced necroptosis of lung tissue, leading to bronchiectasis [65]. Further studies revealed that *Slc11a1* expression in neutrophils exacerbates inflammatory responses, causing damage to various tissues. A study using mouse models of Salmonella-induced colitis demonstrates that *Slc11a1* promotes secretion of proinflammatory cytokines such as IFN-γ, TNF-α, and MIP-1α, intensifying the inflammatory response [66]. Conversely, disruption of *Slc11a1* in Kupffer cells attenuates early-phase warm ischemia–reperfusion injury in mouse livers [67], while its functional loss due to allelic mutations promotes notable tissue repair and wound healing in mouse acute inflammation [68]. In our study, we established that *Slc11a1* mediates vascular endothelial injury through NETs formation. Prior researches have also reported associations between *Slc11a1* and endothelial or vascular injury. *Slc11a1* served as a pivotal gene in neutrophil degranulation, participating in lung epithelial and endothelial damage, thus playing a crucial role in the

pathogenesis of acute respiratory distress syndrome [69]. Upregulation of *Slc11a1* in neutrophils in tissues with antineutrophil cytoplasmic antibody-associated vasculitis tissues fosters vessel wall interactions and platelet activation [70], potentially linked to vascular endothelial damage. Additionally, a study investigating atherosclerosis reported increased *Slc11a1* expression in macrophages from patients, suggesting a potential link between *Slc11a1* upregulation and vascular endothelial damage [71]. These findings support the relationship between *Slc11a1*upregulationin myeloid cells and vascular endothelial damage, aligning with our findings. While numerous studies reported *Slc11a1* upregulation in neutrophils contributing to tissue and cell damage, whether chemotherapy-induced *Slc11a1* upregulation can further damage vascular endothelial cells through additional pathways such as proinflammatory reactions merits further investigation.

Despite the notable strengths of our study, there are limitations that must be acknowledged. First, although we examined indicators of vascular endothelial injury in breast cancer patients and mouse models, we were unable to definitively find morphological evidence linking NETs to endothelial damage. Second, in our *Slc11a1* knockdown experiments in mouse models, we did not achieve targeted knockdown of *Slc11a1* specifically in neutrophils. Third, we have yet to directly elucidate the relationship between NETs-induced vascular endothelial injury and perioperative hypercoagulability or thrombosis in breast cancer patients undergoing neoadjuvant chemotherapy. Lastly, the functional significance of *Slc11a1* in breast cancer patients and its correlation with clinical outcomes remain to be validated.

Conclusions

Our research underscores the capacity of TCb neoadjuvant chemotherapy for breast cancer to augment NETs formation in neutrophils via *Slc11a1*-mediated ROS generation, contributing to vascular endothelial injury. We are confident that the evidence uncovered in this study, demonstrating increased NETs formation during breast cancer neoadjuvant chemotherapy, will facilitate advancements in perioperative therapeutic management strategies for breast cancer patients.

Abbreviations

NET	Neutrophil extracellular trap
MPO	Myeloperoxidase
ROS	Reactive oxygen species
PAD	Peptidylarginine deiminase
dsDNA	Double-stranded DNA
vWF	von Willebrand factor
ELISA	Enzyme-linked immunosorbent assay
FBS	Fetal bovine serum
AAV	Adeno-associated virus
shRNA	Short hairpin RNA
CCK-8	Cell counting Kit-8
q-PCR	Quantitative real-time PCR
DEG	Differentially expressed gene
SD	Standard deviation
ANOVA	Analysis of variance

Supplementary Information

The online version contains supplementary material available at https://doi.org/10.1186/s13058-025-02011-y.

Supplementary material 1.

Supplementary material 2.

Author contributions

L.K., X.Z. and P.X. designed the study. L.K., S.H., Y.Z. and Y.H. performed the experiments. X.X., Y.Y. and X.M. collected the clinical data. L.K. and K.X. analyzed the data. L.K., and X.Z. prepared the manuscript. All authors read and approved the final manuscript.

Funding

This work was supported by the National Natural Science Foundation of China (NO. 32171124, 32471185), the Zhejiang Provincial Medical and Health Science and Technology Plan (NO. 2020KY482, 2025KY701), the Self-Deployed Project Fund of Hangzhou Institute of Medicine, Chinese Academy of Sciences (NO. 2024ZZBS13), and the Cultivation Fund of National Natural Science Foundation of Zhejiang Cancer Hospital (NO. PY2022046).

Availability of data and materials

The datasets used and/or analysed during the current study are available from the corresponding author on reasonable request.

Declarations

Ethics approval and consent to participate

This study was conducted with the approval of the Medical Ethics Committee of Zhejiang Cancer Hospital (Approved No. IRB-2023–751), strictly adhering to the principles outlined in the Declaration of Helsinki. Prior to participation, written informed consent was obtained from all patients or their legal representatives. All experiments involving mice were conducted in accordance with the guidelines set forth by the Animal Review Committee of Zhejiang Cancer Hospital (protocol license number: 2024–02-067).

Consent for publication

Not applicable.

Competing interests

The authors declare that they have no competing interests.

Author details

[1]Department of Anesthesiology, Zhejiang Cancer Hospital; Laboratory of Anethesia and Perioperative Medicine, Hangzhou Institute of Medicine (HIM), Chinese Academy of Sciences, No. 1, East Banshan Road, Hangzhou 310022, Zhejiang, People's Republic of China. [2]Department of Breast Surgery, Zhejiang Cancer Hospital, Hangzhou Institute of Medicine (HIM), Chinese Academy of Sciences, Hangzhou 310022, Zhejiang, People's Republic of China. [3]Department of Head and Neck Surgery, Zhejiang Cancer Hospital, Hangzhou Institute of Medicine (HIM), Chinese Academy of Sciences, Hangzhou 310022, Zhejiang, People's Republic of China. [4]Department of Physiology, Naval Medical University, Shanghai 200433, People's Republic of China.

Received: 28 October 2024 Accepted: 27 March 2025
Published online: 23 April 2025

References

1. Loibl S, Poortmans P, Morrow M, Denkert C, Curigliano G. Breast cancer. Lancet. 2021;397(10286):1750–69.
2. Anderson FJ, Spencer FA. Risk factors for venous thromboembolism. Circulation. 2003;107(23_suppl_1):1–9.
3. Swystun LL, Mukherjee S, Liaw PC. Breast cancer chemotherapy induces the release of cell-free DNA, a novel procoagulant stimulus. J Thromb Haemost. 2011;9(11):2313–21.
4. Levine MN, Gent M, Hirsh J, Arnold A, Goodyear MD, Hryniuk W, de Pauw S. The thrombogenic effect of anticancer drug therapy in women with stage II breast cancer. New Engl J Med. 1988;318(7):404–7.
5. Colling ME, Tourdot BE, Kanthi Y. Inflammation, infection and venous thromboembolism. Circul Res. 2021;128(12):2017–36.
6. Ma Y, Wei J, He W, Ren J. Neutrophil extracellular traps in cancer. Medcomm. 2024;5(8): e647.
7. Qi H, Yang S, Zhang L. Neutrophil extracellular traps and endothelial dysfunction in atherosclerosis and thrombosis. Front Immunol. 2017;8:928.
8. Hazeldine J, Harris P, Chapple IL, Grant M, Greenwood H, Livesey A, et al. Impaired neutrophil extracellular trap formation: a novel defect in the innate immune system of aged individuals. Aging Cell. 2014;13(4):690–8.
9. Kim SW, Davaanyam D, Seol SI, Lee HK, Lee H, Lee J. Adenosine triphosphate accumulated following cerebral ischemia induces neutrophil extracellular trap formation. Int J Mol Sci. 2020;21(20):7668.
10. Zhang Z, Niu R, Zhao L, Wang Y, Liu G. Mechanisms of neutrophil extracellular trap formation and regulation in cancers. Int J Mol Sci. 2023;24(12):10265.
11. Mousset A, Lecorgne E, Bourget I, Lopez P, Jenovai K, Cherfils-Vicini J, et al. Neutrophil extracellular traps formed during chemotherapy confer treatment resistance via TGF-β activation. Cancer Cell. 2023;41(4):757–75.
12. Zhong J, Tang Y. Research progress on the role of reactive oxygen species in the initiation, development and treatment of breast cancer. Prog Biophys Mol Bio. 2024;188:1–18.
13. Yang L, Liu Q, Zhang X, Liu X, Zhou B, Chen J, et al. DNA of neutrophil extracellular traps promotes cancer metastasis via CCDC25. Nature. 2020;583(7814):133–8.
14. Park J, Wysocki RW, Amoozgar Z, Maiorino L, Fein MR, Jorns J, et al. Cancer cells induce metastasis-supporting neutrophil extracellular DNA traps. Sci Transl Med. 2016;8(361):361ra138.
15. Huang D, Chowdhury S, Wang H, Savage SR, Ivey RG, Kennedy JJ, et al. Multiomic analysis identifies CPT1A as a potential therapeutic target in platinum-refractory, high-grade serous ovarian cancer. Cell Rep Med. 2021;2(12): 100471.
16. Szczepaniak P, Siedlinski M, Hodorowicz-Zaniewska D, Nosalski R, Mikolajczyk TP, Dobosz AM, et al. Breast cancer chemotherapy induces vascular dysfunction and hypertension through a NOX4-dependent mechanism. J Clin Invest. 2022;132(13): e149117.
17. Li T, Yue Y, Ma Y, Zhong Z, Guo M, Zhang J, et al. Fasting-mimicking diet alleviates inflammatory pain by inhibiting neutrophil extracellular traps formation and neuroinflammation in the spinal cord. Cell Commun Signal. 2023;21(1):250.
18. Zeng Z, Xia L, Fan S, Zheng J, Qin J, Fan X, et al. Circular RNA CircMAP3K5 acts as a MicroRNA-22-3p sponge to promote resolution of intimal hyperplasia via TET2-mediated smooth muscle cell differentiation. Circulation. 2021;143(4):354–71.
19. Liu YW, Zhang J, Bi W, Zhou M, Li J, Xiong T, et al. Histones of neutrophil extracellular traps induce CD11b expression in brain pericytes via dectin-1 after traumatic brain injury. Neurosci Bull. 2022;38(10):1199–214.
20. Wong SL, Demers M, Martinod K, Gallant M, Wang Y, Goldfine AB, et al. Diabetes primes neutrophils to undergo NETosis, which impairs wound healing. Nat Med. 2015;21(7):815–9.
21. Zhang H, Liu J, Zhou Y, Qu M, Wang Y, Guo K, et al. Neutrophil extracellular traps mediate m(6)A modification and regulates sepsis-associated acute lung injury by activating ferroptosis in alveolar epithelial cells. INT J Biol Sci. 2022;18(8):3337–57.
22. Barnes BJ, Adrover JM, Baxter-Stoltzfus A, Borczuk A, Cools-Lartigue J, Crawford JM, et al. Targeting potential drivers of COVID-19: Neutrophil extracellular traps. J Exper Med. 2020;217(6):e20200652.
23. Hisada Y, Grover SP, Maqsood A, Houston R, Ay C, Noubouossie DF, et al. Neutrophils and neutrophil extracellular traps enhance venous thrombosis in mice bearing human pancreatic tumors. Haematologica. 2020;105(1):218–25.
24. Shi G, Liu L, Cao Y, Ma G, Zhu Y, Xu J, et al. Inhibition of neutrophil extracellular trap formation ameliorates neuroinflammation and neuronal apoptosis via STING-dependent IRE1α/ASK1/JNK signaling pathway in mice with traumatic brain injury. J Neuroinflamm. 2023;20(1):222.
25. Tian R, Abarientos A, Hong J, Hashemi SH, Yan R, Dräger N, et al. Genome-wide CRISPRi/a screens in human neurons link lysosomal failure to ferroptosis. Nat Neurosci. 2021;24(7):1020–34.
26. Wang S, Song Y, Wang Z, Chang X, Wu H, Yan Z, et al. Neutrophil-derived PAD4 induces citrullination of CKMT1 exacerbates mucosal inflammation in inflammatory bowel disease. Cell Mol Immunol. 2024;21(6):620–33.
27. Thiam HR, Wong SL, Wagner DD, Waterman CM. Cellular mechanisms of NETosis. Annu Rev Cell Dev Biol. 2020;36:191–218.
28. Lokken-Toyli KL, Diaz-Ochoa VE, Camacho L, Stull-Lane AR, Van Hecke A, Mooney JP, et al. Vitamin a deficiency impairs neutrophil-mediated control of salmonella via SLC11A1 in mice. Nat Microbiol. 2024;9(3):727–36.
29. Goswami T, Bhattacharjee A, Babal P, Searle S, Moore E, Li M, et al. Natural-resistance-associated macrophage protein 1 is an H+/bivalent cation antiporter. Biochem J. 2001;354(Pt 3):511–9.
30. Forbes JR, Gros P. Iron, manganese, and cobalt transport by Nramp1 (Slc11a1) and Nramp2 (Slc11a2) expressed at the plasma membrane. Blood. 2003;102(5):1884–92.
31. Chong Y, Wang L, Wang B, Gao Z, Lu Y, Deng W, et al. Molecular cloning and functional characterization of the 5′ regulatory region of the SLC11A1 gene from Yaks. Animals. 2023;13(23):3615.
32. Zhang Y, Chen Y, Mou H, Huang Q, Jian C, Tao Y, et al. Synergistic induction of ferroptosis by targeting HERC1-NCOA4 axis to enhance the photodynamic sensitivity of osteosarcoma. Redox Biol. 2024;76: 103328.
33. Golshan M, Cirrincione CT, Sikov WM, Berry DA, Jasinski S, Weisberg TF, et al. Impact of neoadjuvant chemotherapy in stage II–III triple negative breast cancer on eligibility for breast-conserving surgery and breast conservation rates: surgical results from CALGB 40603 (alliance). Annal Surg. 2015;262(3):434–9.
34. Akram M, Iqbal M, Daniyal M, Khan AU. Awareness and current knowledge of breast cancer. Biol Res. 2017;50(1):33.
35. Hisada Y, Mackman N. Cancer-associated pathways and biomarkers of venous thrombosis. Blood. 2017;130(13):1499–506.
36. Walker AJ, West J, Card TR, Crooks C, Kirwan CC, Grainge MJ. When are breast cancer patients at highest risk of venous thromboembolism? A cohort study using English health care data. Blood. 2016;127(7):849–57.
37. Xiang Q, Tao JS, Li JJ, Tian RB, Li XH. What is the role of von Willebrand factor in chronic hepatitis B virus infection to hepatocellular carcinoma: a review article. Ther Adv Chronic Dis. 2022;13:374174259.
38. Terasawa M, Hiramoto K, Uchida R, Suzuki K. Anti-inflammatory activity of orally administered monostroma nitidum rhamnan sulfate against lipopolysaccharide-induced damage to mouse organs and vascular endothelium. Mar Drugs. 2022;20(2):121.
39. Giuliani A, Ramini D, Sbriscia M, Crocco P, Tiano L, Rippo MR, et al. Syndecan 4 is a marker of endothelial inflammation in pathological aging and predicts long-term cardiovascular outcomes in type 2 diabetes. Diabetol Metab Syndr. 2024;16(1):203.
40. Zhu Z, Ling X, Zhou H, Xie J. Syndecan-4 is the key proteoglycan involved in mediating sepsis-associated lung injury. Heliyon. 2023;9(8): e18600.
41. Di Nisio M, van Es N, Büller HR. Deep vein thrombosis and pulmonary embolism. Lancet. 2016;388(10063):3060–73.
42. Ling S, Xu JW. Phenotypes and functions of "aged" neutrophils in cardiovascular diseases. Biomed Pharmacother. 2024;179: 117324.
43. Chen PJ, Chen SH, Chen YL, Wang YH, Lin CY, Chen CH, et al. Ribociclib leverages phosphodiesterase 4 inhibition in the treatment of neutrophilic inflammation and acute respiratory distress syndrome. J Adv Res. 2024;62:229–43.
44. Gupta R, Kadhim MM, Turki JA, Qasim AM, Alsaikhan F, Khalimovna MN, et al. The interactions of docetaxel with tumor microenvironment. Int Immunopharmacol. 2023;119: 110214.
45. Bhagat A, Shrestha P, Kleinerman ES. The innate immune system in cardiovascular diseases and its role in doxorubicin-induced cardiotoxicity. Int J Mol Sci. 2022;23(23):14649. https://doi.org/10.3390/ijms232314649.
46. Rutecki S, Pakuła-Iwańska M, Leśniewska-Bocianowska A, Matuszewska J, Rychlewski D, Uruski P, et al. Mechanisms of carboplatin- and

paclitaxel-dependent induction of premature senescence and pro-cancerogenic conversion of normal peritoneal mesothelium and fibroblasts. J Pathol. 2024;262(2):198–211.
47. Khan MA, D'Ovidio A, Tran H, Palaniyar N. Anthracyclines suppress both NADPH oxidase- dependent and -independent NETosis in human neutrophils. Cancers. 2019;11(9):1328.
48. Cao C, Yu P, Chu C, Wang Z, Xu W, Cheng F, et al. Magnesium hydride attenuates intestinal barrier injury during hemorrhage shock by regulating neutrophil extracellular trap formation via the ROS/MAPK/PAD4 pathway. Int Immunopharmacol. 2024;130: 111688.
49. Byun DJ, Lee J, Ko K, Hyun YM. NLRP3 exacerbates EAE severity through ROS-dependent NET formation in the mouse brain. Cell Commun Signal. 2024;22(1):96.
50. Kong J, Deng Y, Xu Y, Zhang P, Li L, Huang Y. A two-pronged delivery strategy disrupting positive feedback loop of neutrophil extracellular traps for metastasis suppression. ACS Nano. 2024;18(24):15432–51. https://doi.org/10.1021/acsnano.3c09165.
51. Yang LY, Shen XT, Sun HT, Zhu WW, Zhang JB, Lu L. Neutrophil extracellular traps in hepatocellular carcinoma are enriched in oxidized mitochondrial DNA which is highly pro-inflammatory and pro-metastatic. J Cancer. 2022;13(4):1261–71.
52. Giannakopoulos S, Park J, Pak J, Tallquist MD, Verma S. Post-COVID pulmonary injury in K18-hACE2 mice shows persistent neutrophils and neutrophil extracellular trap formation. Immun Inflamm Dis. 2024;12(8): e1343.
53. Yu M, Li X, Xu L, Zheng C, Pan W, Chen H, et al. Neutrophil extracellular traps induce intrahepatic thrombotic tendency and liver damage in cholestatic liver disease. Hepatol Commun. 2024;8(8):e0513.
54. Liang Y, Lin J, Huang B, Weng M, Zhen T, Yang L, et al. NET-related gene as potential diagnostic biomarkers for diabetic tubulointerstitial injury. J Diabetes Res. 2024;2024:4815488.
55. Zhao P, Zhu J, Bai L, Ma W, Li F, Zhang C, et al. Neutrophil extracellular traps induce pyroptosis of pulmonary microvascular endothelial cells by activating the NLRP3 inflammasome. Clin Exp Immunol. 2024;217(1):89–98.
56. Misra DP, Thomas KN, Gasparyan AY, Zimba O. Mechanisms of thrombosis in ANCA-associated vasculitis. Clin Rheumatol. 2021;40(12):4807–15.
57. Sun LL, He HY, Li W, Jin WL, Wei YJ. The solute carrier transporters (SLCs) family in nutrient metabolism and ferroptosis. Biomark Res. 2024;12(1):94.
58. Hsu HC, Lee YS, Imbang TI, Liu TC, Hung SI. SLC11A1 predicts the overall survival of patients with colorectal cancer. AM J Cancer Res. 2024;14(6):2839–51.
59. Cellier M. Developmental control of NRAMP1 (SLC11A1) expression in professional phagocytes. Biology. 2017;6(2):28.
60. Niemiec MJ, De Samber B, Garrevoet J, Vergucht E, Vekemans B, De Rycke R, et al. Trace element landscape of resting and activated human neutrophils on the sub-micrometer level. Metallomics. 2015;7(6):996–1010.
61. Co H, Wu CC, Lee YC, Chen SH. Emergence of large-scale cell death through ferroptotic trigger waves. Nature. 2024;631(8021):654–62.
62. Choi EJ, Jeon CH, Lee IK. Ferric ammonium citrate upregulates PD-L1 expression through generation of reactive oxygen species. J Immunol Res. 2022;2022:6284124.
63. Fritsche G, Nairz M, Libby SJ, Fang FC, Weiss G. Slc11a1 (Nramp1) impairs growth of Salmonella enterica serovar typhimurium in macrophages via stimulation of lipocalin-2 expression. J Leukocyte Biol. 2012;92(2):353–9.
64. Redmond SB, Chuammitri P, Andreasen CB, Palić D, Lamont SJ. Genetic control of chicken heterophil function in advanced intercross lines: associations with novel and with known Salmonella resistance loci and a likely mechanism for cell death in extracellular trap production. Immunogenetics. 2011;63(7):449–58.
65. Qian H, Ge A, Jiang JJ, Xu JF. Necroptosis-related subtypes are associated with bronchiectasis in pulmonary non-tuberculous mycobacteria-infected patients: a perspective based on transcriptomic analysis. Eur J Clin Microbiol. 2023;42(2):141–52.
66. Valdez Y, Grassl GA, Guttman JA, Coburn B, Gros P, Vallance BA, et al. Nramp1 drives an accelerated inflammatory response during Salmonella-induced colitis in mice. Cell Microbiol. 2009;11(2):351–62.
67. Wyllie S, Seu P, Gao FQ, Gros P, Goss JA. Disruption of the Nramp1 (also known as Slc11a1) gene in Kupffer cells attenuates early-phase, warm ischemia-reperfusion injury in the mouse liver. J Leukocyte Biol. 2002;72(5):885–97.
68. De Franco M, Carneiro PS, Peters LC, Vorraro F, Borrego A, Ribeiro OG, et al. Slc11a1 (Nramp1) alleles interact with acute inflammation loci to modulate wound-healing traits in mice. Mamm Genome. 2007;18(4):263–9.
69. Hu L, Zhao T, Sun Y, Chen Y, Bai K, Xu F. Bioinformatic identification of hub genes and key pathways in neutrophils of patients with acute respiratory distress syndrome. Medicine. 2020;99(15): e19820.
70. Friedman MA, Choi D, Planck SR, Rosenbaum JT, Sibley CH. Gene expression pathways across multiple tissues in antineutrophil cytoplasmic antibody-associated vasculitis reveal core pathways of disease pathology. J Rheumatol. 2019;46(6):609–15.
71. Hägg DA, Jernås M, Wiklund O, Thelle DS, Fagerberg B, Eriksson P, et al. Expression profiling of macrophages from subjects with atherosclerosis to identify novel susceptibility genes. Int J Mol Med. 2008;21(6):697–704.

Publisher's Note